Functional validation of the anaplastic lymphoma kinase signature identifies *CEBPB* and *BCL2A1* as critical target genes

Roberto Piva,[1] Elisa Pellegrino,[1] Michela Mattioli,[2] Luca Agnelli,[2] Luigia Lombardi,[2] Francesco Boccalatte,[1] Giulia Costa,[1] Bruce A. Ruggeri,[3] Mangeng Cheng,[3] Roberto Chiarle,[1] Giorgio Palestro,[1] Antonino Neri,[2] and Giorgio Inghirami[1,4]

[1]Department of Pathology and Center for Experimental Research and Medical Studies (CeRMS), University of Turin, Turin, Italy. [2]Laboratory of Experimental Hematology and Molecular Genetics, Ospedale Maggiore Istituto di Ricovero e Cura a Carattere Scientifico, Milan, Italy. [3]Oncology, Cephalon Inc., West Chester, Pennsylvania, USA. [4]Department of Pathology and New York University Cancer Institute, New York University School of Medicine, New York, New York, USA.

Anaplastic large cell lymphomas (ALCLs) represent a subset of lymphomas in which the *anaplastic lymphoma kinase* (*ALK*) gene is frequently fused to the *nucleophosmin* (*NPM*) gene. We previously demonstrated that the constitutive phosphorylation of ALK chimeric proteins is sufficient to induce cellular transformation in vitro and in vivo and that ALK activity is strictly required for the survival of ALK-positive ALCL cells. To elucidate the signaling pathways required for ALK-mediated transformation and tumor maintenance, we analyzed the transcriptomes of multiple ALK-positive ALCL cell lines, abrogating their ALK-mediated signaling by inducible ALK RNA interference (RNAi) or with potent and cell-permeable ALK inhibitors. Transcripts derived from the gene expression profiling (GEP) analysis uncovered a reproducible signature, which included a novel group of ALK-regulated genes. Functional RNAi screening on a set of these ALK transcriptional targets revealed that the transcription factor C/EBPβ and the antiapoptotic protein BCL2A1 are absolutely necessary to induce cell transformation and/or to sustain the growth and survival of ALK-positive ALCL cells. Thus, we proved that an experimentally controlled and functionally validated GEP analysis represents a powerful tool to identify novel pathogenetic networks and validate biologically suitable target genes for therapeutic interventions.

Introduction

Anaplastic large cell lymphomas (ALCLs) represent a subset of non-Hodgkin lymphomas characterized by unique cell morphology and expression of CD30. They constitute approximately 5% of all large cell lymphomas in adults and more than 25% in children. Despite their relatively low incidence, the interest in ALCL has been constantly growing since the discovery of their recurrent cytogenetic defects (1). A discrete subset of ALCLs is characterized by specific chromosome translocations, in which the *anaplastic lymphoma kinase* (*ALK*) gene, on chromosome 2, is fused to several partners, most frequently to the *nucleophosmin* (*NPM*) gene (2, 3). The presence of ALK fusions in inflammatory myofibroblastic tumors as well as lymphoma implies that ALK is involved in oncogenesis of both nonhematopoietic and hematopoietic tumors (4). Moreover, the deregulated expression of the ALK receptor has been documented in a subset of nonlymphoid tumors, including sarcomas, neuroblastomas, and gliomas (5–7). The *ALK* gene encodes a tyrosine kinase receptor, whose physiologic expression in mammals is largely limited to specific regions of the central and the peripheral nervous system (8, 9). ALK fusion proteins maintain the intracytoplasmic tail of the ALK receptor at their C terminus. This region contains a catalytic domain, whereas the N-terminal region of all fusion proteins has dimerization domains. As a consequence of dimerization, ALK chimeras undergo autophosphorylation and become constitutively active. We have previously demonstrated that the constitutive expression and phosphorylation of NPM-ALK are sufficient for cellular transformation in vitro and for the development of lymphoid neoplasia in transgenic mice (10). Moreover, ALK activity is strictly required for the survival of ALCL cells in vitro and in vivo (11, 12). However, the precise mechanisms by which NPM-ALK mediates cellular transformation and its requirements for tumor growth and survival are still unclear. Activated ALK chimeras bind multiple adaptor proteins capable of firing different pathways regulating cell proliferation, survival, and transformation (4, 13, 14). The known adaptors include Grb2, Shc, IRS-1, phospholipase Cγ (PLC-γ) PI3K, and Jak3, which activate numerous downstream molecules, including cyclin D, ERK1/2, STAT, and AKT (3, 14–16). By using cell lineage–specific conditional knockout models, we demonstrated that the genetic ablation of STAT3 in ALK-positive cells leads to cell death and prevents the generation of B cell neoplasms (17). PLC-γ and AKT have been shown to play an essential role in ALK-mediated transformation in vitro (15, 18, 19). It has been postulated that the activation of Ras/ERK and PLC-γ pathways contributes to the enhancement of cell growth and that STAT3 and PI3K/AKT play a major role in inhibiting apoptosis. Nevertheless, it is conceivable that ALK-mediated transformation requires a more complex scenario. Comprehensive analyses of the transcriptome of ALK-positive ALCLs are limited and derived from a small number of fresh tissues or ALK-positive cell lines (20–23). Since ALCL cells often represent a minority within pathological samples and the normal

Nonstandard abbreviations used: ALCL, anaplastic large cell lymphoma; ALK, anaplastic lymphoma kinase; *BCL2A1*, *B-cell leukemial lymphoma2 related protein A1*; C/EBPβ, CCAAT/enhancer-binding protein β; GEP, gene expression profile/profiling; MEF, mouse embryonic fibroblast; *NPM*, *nucleophosmin*; PLC-γ, phospholipase Cγ; RNAi, RNA interference; shRNA, short hairpin RNA.

Conflict of interest: The authors have declared that no conflict of interest exists.

Citation for this article: *J. Clin. Invest.* **116**:3171–3182 (2006). doi:10.1172/JCI29401.

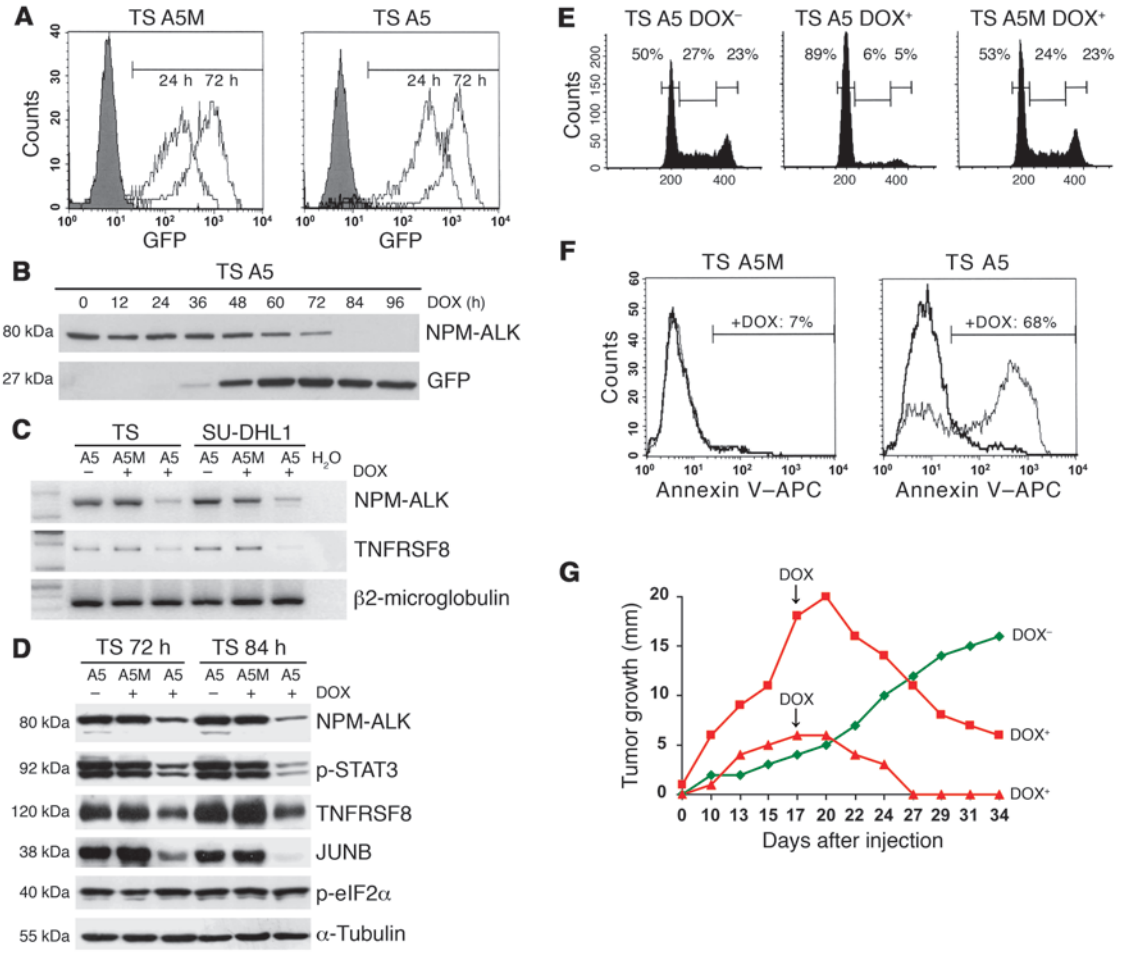

Figure 1

Inducible NPM-ALK knock down leads to apoptosis of ALCL cells and tumor regression in vivo. (**A**) Conditional expression of the shRNA internal marker gene GFP. TS cells cotransduced with pLV-tTR-KRAB/DsRed and pLVTH-ALK-A5/GFP (TS A5, right) or with the mutated pLVTH-ALK-A5M/GFP (TS A5M, left) lentiviral preparations were cultured with doxycycline (DOX) (1 μg/ml) for the indicated times and subsequently analyzed by flow cytometry (72 hours). (**B**) Kinetics of NPM-ALK knock down. TS-TTA-A5 cells were treated with DOX and harvested at the indicated times. Whole-cell lysates were analyzed by Western blotting with anti-GFP or ALK antibodies. (**C** and **D**) Inducible NPM-ALK knock down leads to downmodulation of ALK and of known downstream targets in TS-TTA-A5 cells. (**C**) RNA levels of *NPM-ALK*, *CD30* (*TNFRSF8*), and *β2-microglobulin* transcripts were determined by semiquantitative RT-PCR (72 hours). (**D**) Protein expressions were assayed by Western blotting with the specified antibodies (72–84 hours). (**E** and **F**) Loss of NPM-ALK leads to G_1 cell-cycle arrest and apoptosis. TS-TTA-A5 or -A5M cells were harvested after DOX induction and analyzed by flow cytometry. (**E**) The percentage of cells in G_0/G_1, S, and G_2-M phases was determined by PI staining (96 hours). (**F**) The fraction of apoptotic cells was assayed by annexin V staining (120 hours). (**G**) NPM-ALK ablation induces tumor regression in vivo. Representative tumor growth curves for TS-TTA-A5 cells injected subcutaneously into BNX mice in an untreated mouse (green) or 2 mice treated for 14 days with DOX (red) starting at day 17. Each data point represents the average diameter of 2 tumor masses. Similar results were obtained from 9 mice injected with TS-TTA-A5 cells, with slightly differing kinetics.

counterpart of ALCL cells is not known, these studies could not be considered paradigmatic.

To clarify the precise mechanisms and signaling pathways required for ALK-mediated transformation and tumor growth, we analyzed transcriptomes of ALK-positive ALCL cell lines using tightly controlled experimental conditions, in which the ALK signaling was abrogated by an inducible ALK short hairpin RNA (shRNA) or by potent small-molecule ALK inhibitors. These approaches provided a bona fide ALK oncogenic signature by filtering out the majority of off-target effects triggered by each experimental system. Some of the positive hits were functionally validated by RNA interference (RNAi) to ascertain genes that provide growth and survival benefits to tumor cells. Our studies demonstrated that *B-cell leukemial lymphoma2 related protein A1*, (*BCL2A1*) and the transcription factor CCAAT/enhancer-binding protein β (C/EBPβ) are regulated by NPM-ALK activity and are absolutely necessary for sustaining the survival and growth of ALK-positive ALCL cells. These studies confirm that combined approaches will ultimately disclose the pathogenetic networks in human cancers, paving the way for the discovery of new targets for alternative therapeutic strategies.

Results

Inducible NPM-ALK silencing leads to cell cycle arrest and apoptosis in vitro and tumor growth regression in vivo. Using a lentivirus-medi-

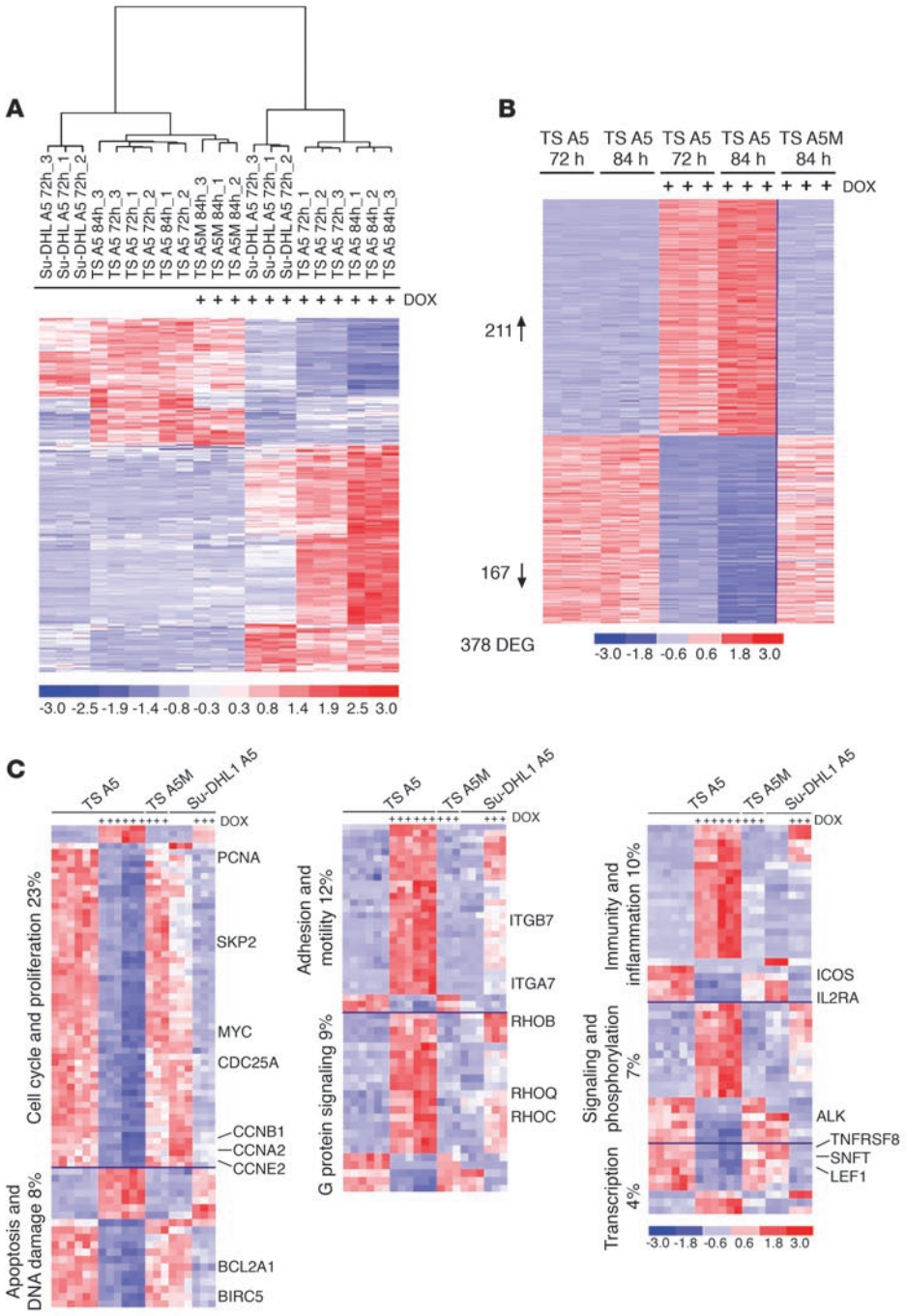

Figure 2
NPM-ALK gene expression signature in ALCL cells derived by inducible shRNA. (**A**) GEP differentiates ALCL cells based on ALK expression. Unsupervised analysis of TS-TTA-A5, TS-TTA-A5M, and Su-DHL1-TTA-A5 cells untreated or treated with DOX for the indicated times. In the matrix, each column represents a sample, and each row a gene. The 21 samples were grouped according to the expression levels of the 267 most variable genes, after removal of the signals whose expression levels did not vary across experimental conditions. The color scale bar represents relative gene expression changes, normalized by the standard deviation. (**B**) The supervised analysis identified a selected number of genes specifically modified in untreated versus treated TS-TTA-A5 cells. Cell samples were cultured with (n = 6) and without (n = 6) DOX for the indicated times. The expression pattern of the identified genes in TS-TTA-A5M cells treated with DOX (84 hours) is shown on the right side. DEG, differentially expressed genes. (**C**) Functional stratification of ALK-regulated genes. Genes differentially expressed in TS-TTA-A5 treated with DOX were grouped according to their functional categories.

ated ALK-knockdown and small-molecule approach, we recently demonstrated that ALK is required for the maintenance of the neoplastic phenotype of ALCL and represents a suitable target for specific pharmacological therapies (11, 12). Here, we exploited an inducible RNAi method to unveil new ALK oncogenic pathways. To identify candidate genes involved in the pathogenesis of ALCL, we enforced the expression of an ALK-A5 shRNA under a tightly regulated doxycycline-controllable transcriptional repressor in multiple ALCL cell lines, including TS and Su-DHL1. This strategy allowed for highly reproducible NPM-ALK silencing. Transduction of the ALK-A5 or mutated ALK-A5M shRNA sequences was accomplished using lentiviral vectors carrying a GFP reporter. Following doxycycline treatment, ALK-A5 and -A5M shRNA constructs were expressed in human ALCL cells, leading to the downmodulation of both NPM-ALK mRNA and protein expression (Figure 1, A–C). The inhibition of the NPM-ALK signaling was coupled to the repression of CD30 (TNFRSF8) and JunB expression (ref. 24 and Chiarle et al., manuscript submitted for publication) and the reduction of STAT3 phosphorylation, in the absence of detectable changes of eIF2α phosphorylation, a marker of double-stranded RNA–induced (dsRNA-induced) interferon response (Figure 1, C and D). Conditional NPM-ALK knock down was coupled to a G_1 cell-cycle arrest and followed by apoptosis (Figure 1, E and F). To determine whether this system could abrogate NPM-ALK–driven growth in

vivo, we studied the growth patterns of xenograft tumors. TS-TTA-A5 cells, injected subcutaneously into the flanks of BNX mice, formed visible growing tumors after 2–3 weeks latency. In mice treated with doxycycline, tumor growth rapidly diminished compared with untreated mice; after 10 days most tumors were reabsorbed, and eventually mice became tumor free (Figure 1G) even upon removal of doxycycline (up to 2 months; data not shown). Overall, the inducible ALK shRNA approach allowed us to corroborate the strict requirement of ALK signaling for the survival of ALK-positive ALCL cells, and it represents an ideal tool to untangle the NPM-ALK gene expression signature.

NPM-ALK gene expression signature in ALCL cells. To identify reproducible signatures in multiple ALCL cell lines, we compared the gene expression profile (GEP) of 2 ALCL cell lines, TS and Su-DHL1, prior to and after doxycycline-mediated ALK knock down. Samples from 3 independent replicas were processed and hybridized to Affymetrix U133A gene chips. As controls, we used untreated cells and transduced TS cells with a mutated ALK shRNA construct (A5M). To determine whether the GEP of ALCL cell lines could identify distinct groups based on NPM-ALK expression, we performed an unsupervised analysis (25). The 21 samples generated a dendrogram with 2 major branches: one contained all control samples expressing NPM-ALK (A5 shRNA uninduced and A5M shRNA induced for 84 hours); the second branch grouped only samples in which A5 shRNA was induced (Figure 2A). The quantification of changes in *ALK* transcripts after RNAi showed that *ALK* levels decreased an average of 8.2-fold in TS cells and 4.7-fold in Su-DHL1 cells. Many transcripts whose expression is known to be regulated by NPM-ALK were exclusively enlisted among these groups. These included *CD30* (*TNFRSF8*), *JUNB*, *MYC*, *survivin* (*BIRC5*), *p21* (*CDKN1A*), and *p27* (*CDKN1B*) (Supplemental Figure 1, A and B; supplemental material available online with this article; doi:10.1172/JCI29401DS1). On the contrary, the expression of classic interferon target genes (e.g., *OAS1*) was not significantly modulated after RNAi (Supplemental Figure 1C). To validate the specificity of the NPM-ALK signature, we analyzed the expression profile upon induction of the mutated ALK-A5M shRNA. The GEPs comparison of ALK-A5M with untreated cell samples detected only 23 genes consistently modified (4% compared to 600 genes modulated with A5 at the same time point [23 × 100/600 = 3.833%]; Supplemental Figure 1D). Overall, these findings strongly suggest that changes observed after ALK shRNA induction were due to the knock down of ALK signaling and were distinct from a general activation signature in response to exogenous dsRNA or to doxycycline treatment. Genes differentially expressed within the 2 major groups were subsequently characterized by a supervised analysis. The resulting NPM-ALK gene expression signature in TS cells revealed a total of 345 probe sets differentially expressed upon 72 hours of A5 shRNA induction, which increased to 600 at 84 hours. Interestingly, the analysis of these profiles showed that nearly all genes modulated at 84 hours were also concordantly modified at 72 hours, though to a lesser degree. Moreover, the analysis of all TS samples, without any temporal segregation, revealed a more restricted cluster, with a total of 378 transcripts (211 upregulated and 167 downregulated) (Figure 2B). To functionally stratify these genes and to predict their putative pathogenetic properties, we assigned them to functional categories. Overrepresented genes included those related to cell cycle (23%), apoptosis and DNA damage (8%), adhesion and motility (12%), G protein signaling (9%), and inflammation and immune response (10%) (Figure 2C).

To further validate the NPM-ALK signature, we performed a second GEP analysis in the Su-DHL1 cell line, where 149 transcripts were found to be differentially expressed (Supplemental Figure 2A). A comparison of the signatures showed that 69% of transcripts (103 genes) were shared by the 2 cell lines (72 increased and 31 decreased) (Supplemental Figure 2B).

Validation of NPM-ALK signature in ALCL cells by ALK inhibitors. To validate the GEP signature obtained after RNAi, and to exclude possible bias due to potential off-targets aberrantly modulated by ALK-A5 shRNA, we took advantage of cell-permeable pyrrolocarbazole-derived ALK inhibitors (A2 and A3) (12). These inhibitors have potent anti-ALK activity both in vitro and in cell-based assays. We first confirmed their efficacy in inhibiting ALK-dependent biochemical and biological activities in a panel of ALK-positive cell lines including TS by demonstrating proapoptotic effects in ALK-positive cells with a minimal cellular cytotoxicity toward ALK-negative cells (Figure 3A and data not shown). A structurally similar compound (A1), which displays no or weak ALK inhibitory activity up to 30 μM in cells, was used as a negative control (12). To diminish cell line–dependent gene expression heterogeneity, we performed all transcriptional experiments in TS-TTA-A5 cells, the same type as was used in the inducible shRNA GEP experiments. GEP studies were performed with samples obtained 6 hours after treatment, based on the downregulation of known NPM-ALK transcriptional targets such as *JUNB* and *TNFRSF8*, in the absence of any detectable commitment to apoptosis (Figure 3A and data not shown). The unsupervised analysis generated a dendrogram with 2 major branches established exclusively on the NPM-ALK activity (Figure 3B). In addition, the supervised analysis of the cells treated with the 2 ALK inhibitors versus untreated cells and ALK-negative compound–treated cells revealed a total of 268 differentially expressed transcripts, many of which were identified and modulated accordingly (Figure 3C).

To identify a stronger and more reliable NPM-ALK signature, we compared the differentially expressed genes, identified by the supervised analysis following either ALK silencing or kinase inhibition, and selected only the overlapping genes. A total of 52 common transcripts (22 upregulated and 30 downregulated) were identified (Figure 3D and Supplemental Table 1). To provide evidence for the reliability of this combined NPM-ALK signature, we arbitrarily selected 6 targets (*ICOS*, *RGS16*, *CCL20*, *DKC1*, *GNL3*, *BCL2A1*) and verified their transcript expression by semiquantitative RT-PCR in the presence or absence of ALK silencing. We found that the expression of all selected targets was specifically downregulated in multiple ALK-positive cells, including TS and Su-DHL1, following NPM-ALK knock down or kinase inhibition (Figure 3E and data not shown).

BCL2A1 expression is regulated by NPM-ALK activity and sustains the survival of ALK-positive ALCL cells. To dissect the biological properties of the 6 ALK-regulated genes (*ICOS*, *RGS16*, *CCL20*, *DKC1*, *GNL3*, *BCL2A1*), we used an RNAi approach. We reasoned that if any of these genes acts as an oncogene and/or plays a relevant role in the maintenance of the ALCL neoplastic phenotype, its loss could be sufficient to affect cell survival, proliferation, or morphology, despite sustained ALK signaling. We cloned multiple shRNA sequences (4–5) specific for each target into a lentiviral EGFP vector and transduced them individually into ALCL cells. For all 6 genes, at least 1 shRNA sequence reproducibly decreased transcript levels more than 4-fold (data not shown). Once the biological effects of the transduction of TS cells were tested, a remarkable

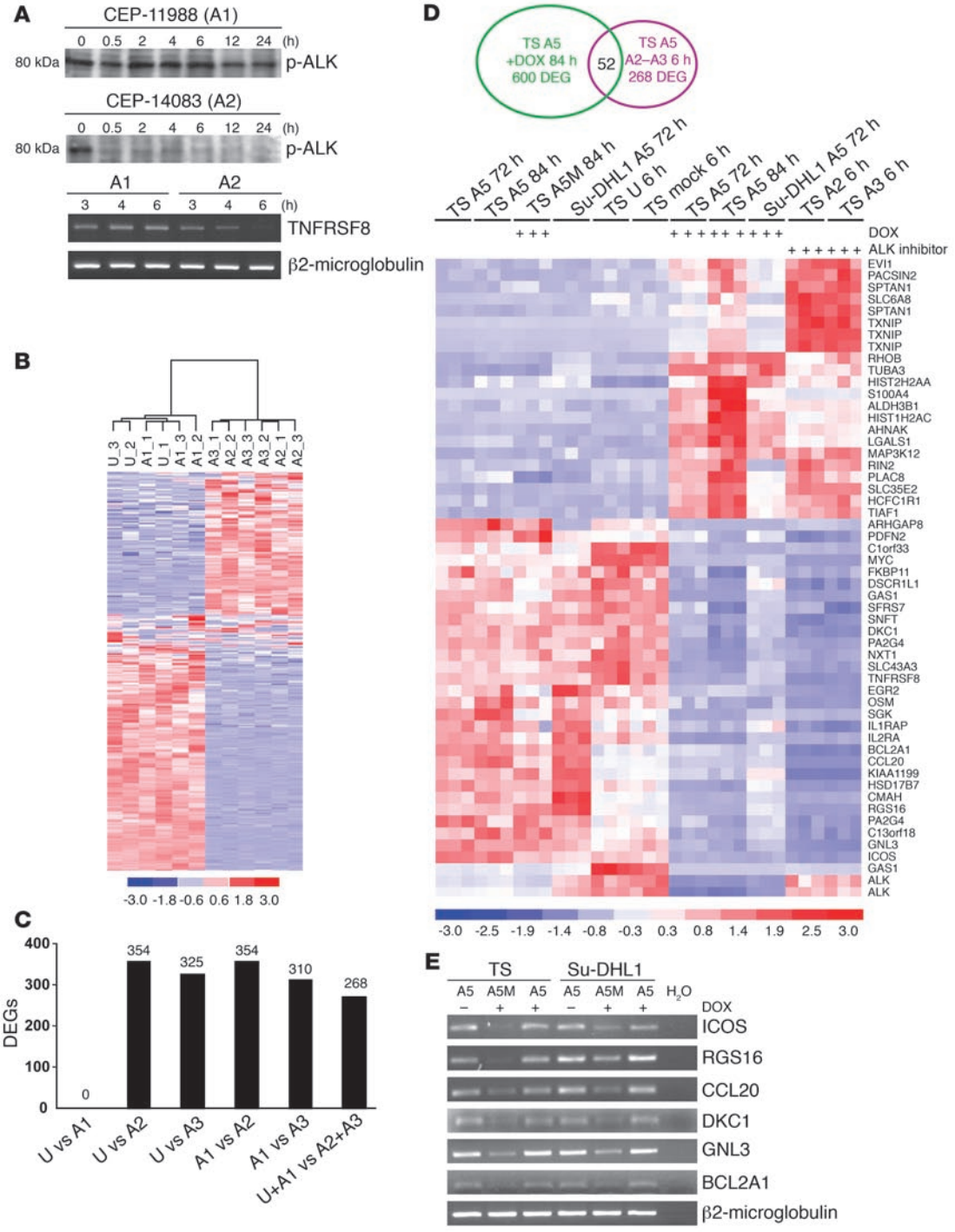

Figure 3

Generation and validation of a restricted signature for ALK-positive ALCL cells. (**A**) Kinetics of NPM-ALK dephosphorylation and *CD30* (*TNFRSF8*) downregulation determined by ALK inhibitors. ALK-positive cells were treated (300 nM) with A1 (CEP-11988) or A2 (CEP-14083) as indicated. ALK phosphorylation was assayed using a specific phospho-ALK (Y1604) antibody (upper panels). Levels of *TNFRSF8* and *β2-microglobulin* mRNA were analyzed by semiquantitative RT-PCR (lower panels). (**B**) Gene expression profiling differentiates ALCL cells based on ALK activity. Unsupervised analysis of TS-TTA-A5 cells after no treatment (U) or treatment with A1, A2, or A3 (CEP-14513) ALK inhibitors (6 hours). In the matrix, each column represents a sample and each row a gene. The 12 samples were grouped in the dendrogram according to the expression levels of the 320 most variable genes. (**C**) ALK inhibitors modulate a similar set of genes. Number of genes differentially expressed in TS-TTA-A5 following ALK kinase inhibition as determined by supervised analysis for the indicated conditions. (**D**) Eisen plot of the expression values of 52 transcripts consistently modulated across shRNA- and ALK inhibitor-treated TS-TTA-A5 cells. (**E**) RT-PCR validation of NPM-ALK signature. A5- or A5M-transduced TS-TTA and Su-DHL1-TTA cells were treated with DOX for 72 hours, and mRNA expression for 6 genes (*ICOS, RGS16*, *CCL20*, *DKC1*, *GNL3*, *BCL2A1*) was determined by semiquantitative RT-PCR.

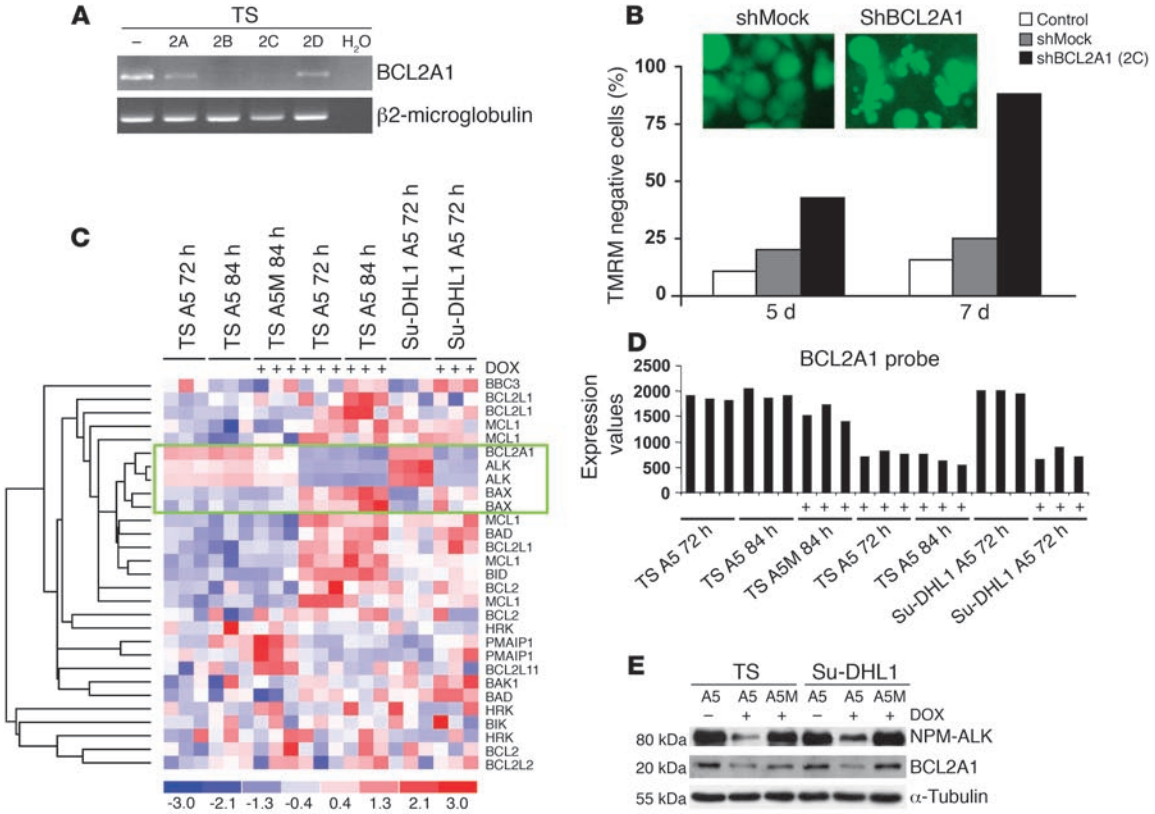

Figure 4

BCL2A1 expression is regulated by NPM-ALK activity and sustains the survival of ALK-positive ALCL cells. (**A** and **B**) BCL2A1 shRNA induces apoptosis of ALCL cells. (**A**) TS cells were transduced with lentivirus (pLKO-GFP) expressing 4 BCL2A1-directed shRNAs (2A–D). *BCL2A1* mRNA expression was determined by RT-PCR analysis (72 hours). (**B**) TS cells were transduced with a mock or a BCL2A1-directed shRNA (2C), and the percentage of apoptotic cells was determined by tetramethylrodamine methyl ester (TMRM) staining 5 and 7 days after infection. Cell morphology of BCL2A1- and mock shRNA–transduced TS cells is shown in the inset. These findings are representative of 3 independent experiments. (**C**–**E**) BCL2A1 expression correlates with ALK signaling. (**C**) The expression of *BCL2* family genes was evaluated in all experimental conditions (33 samples) for absolute correlation with *ALK*. The *BCL2A1* gene clustered within the branch including the *ALK* probe set (green rectangle). (**D**) *BCL2A1* mRNA expression is significantly downmodulated after ALK RNAi. mRNA expression levels were assessed by microarray analysis of ALK-knockdown experiments in TS and Su-DHL1 cells. (**E**) Loss of ALK expression leads to the BCL2A1 protein downregulation. TS-TTA and Su-DHL1-TTA cells transduced with A5 or A5M were treated with DOX (84 hours). Western blot analysis was carried out on whole-cell lysates with antibodies against BCL2A1 and ALK.

apoptotic phenotype was observed in cells transduced with shRNA for BCL2A1 (Figure 4, A and B). The *BCL2A1* cluster gene belongs to the *BCL2* family of antiapoptotic genes and includes 3 members (A1a, A1b, A1d). It has been shown to regulate T cell survival (26) and to be overexpressed in some leukemic cells (27). By clustering the expression profile of all *BCL2* family members following ALK silencing, we found that *BCL2A1* transcripts had the highest degree of correlation to ALK (Figure 4C). The downregulation of the *BCL2A1* mRNA was similar in TS and Su-DHL1 cells (Figure 4, C and D) and was confirmed by the parallel decrease in the BCL2A1 protein levels after ALK silencing (Figure 4E). Western blotting performed on a panel of ALCL and other hematopoietic cell lines demonstrated that BCL2A1 protein expression was not restricted to ALCL cells; however, ALK-positive cells preferentially expressed BCL2A1 among the antiapoptotic *BCL2* family genes. Moreover, loss of BCL2A1 via shRNA was also sufficient to induce apoptosis in ALK-negative hematopoietic cells (data not shown). Overall, these findings unveiled a specific ALK-mediated regulation of a member of the *BCL2* family and demonstrated that BCL2A1 plays an important role in the survival of ALCL cells. Since BCL2A1 is not restricted to ALCL, its tumorigenic role may be more general, making this protein an appealing target for cancer therapy.

C/EBPβ is an NPM-ALK target required for ALK-mediated transformation and growth. To discover novel NPM-ALK targets, a second strategy aimed to identify genes whose expression strongly correlated with the modulation of ALK function was employed. Since the mRNA expression of *ALK* was not changed when ALK inhibitors were used, we selected the NPM-ALK–induced gene *TNFRSF8* (CD30) as a reference. The list of genes obtained from GEP of ALK inhibitors was hierarchically clustered for correlation in all experimental conditions (33 independent samples). The TNFRSF8 branch comprised transcripts previously annotated among overlapping genes such as *JUNB*, *DKC1*, *SNFT*, *PA2G4*, *SLC43A3*, *NXT1*, and novel genes (compare Figure 3D with Figure 5A). These included *DDX21*, *NOL5A*, and *CEBPB*, which had the highest *z* scores (–11.2, –11.8, and –9.5, respectively).

The transcription factor C/EBPβ (28) is of particular interest since it is abundantly expressed in Hodgkin lymphoma and ALCL

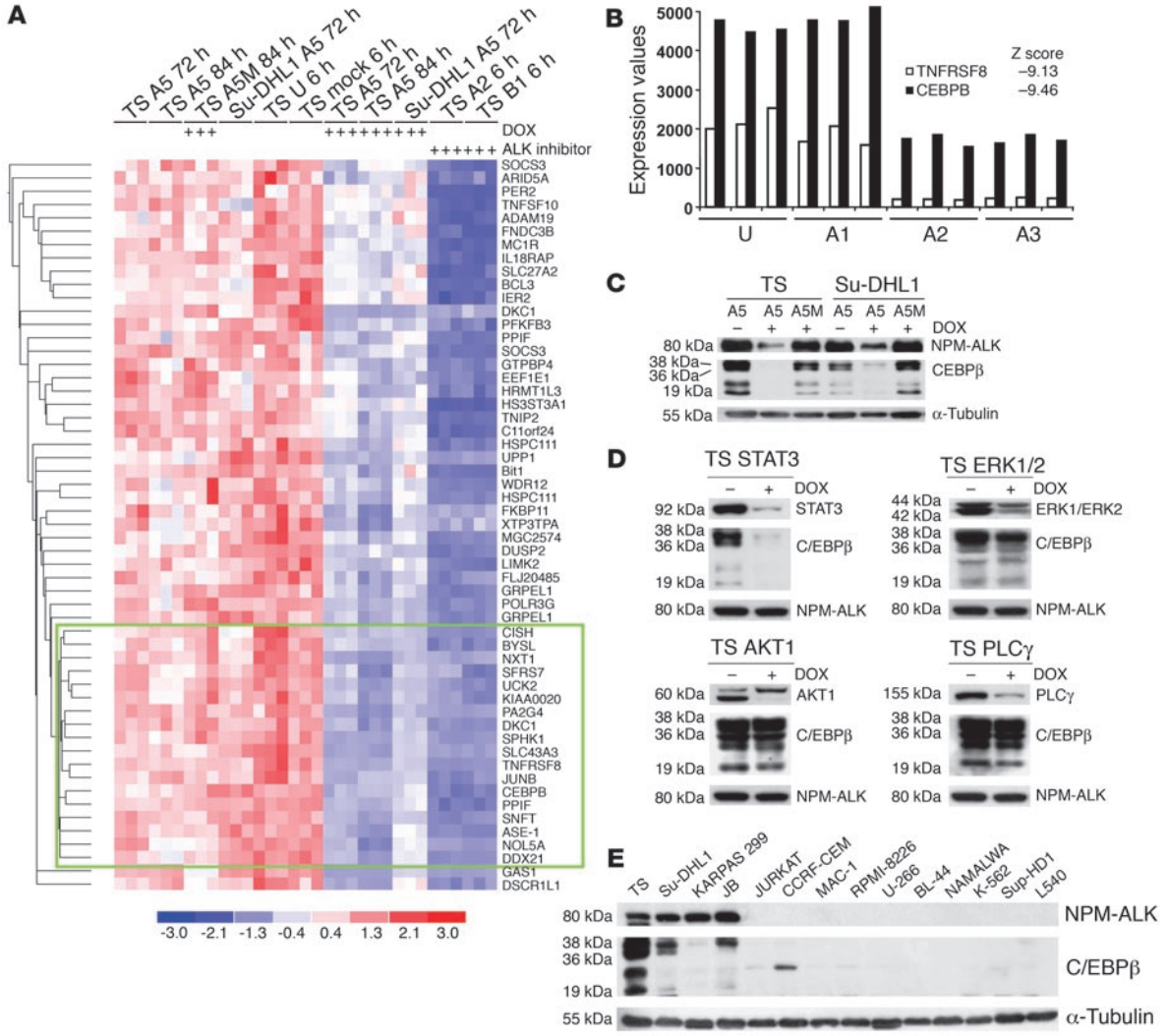

Figure 5

CEBPB is an NPM-ALK and STAT3 target gene. (**A**) Identification of genes whose expression strongly correlated with *TNFRSF8* expression. Genes from the list obtained by the supervised analysis of TS-TTA-A5 (untreated+A1) versus A2+A3 cells (268 genes) were hierarchically clustered in all experimental conditions (33 samples). The plot represents a portion of the list, which includes transcripts with the highest degree of correlation to TNFRSF8 expression (green rectangle). (**B**) *CEBPB* expression is correlated with *TNFRSF8*. *TNFRSF8* and *CEBPB* mRNA expression levels are represented in the histogram as assessed by microarray analysis of 12 TS-TTA-A5 samples. The statistical significance was ranked according to the *z* score. (**C**) C/EBPβ protein expression is strongly repressed following NPM-ALK silencing. TS-TTA and Su-DHL1-TTA cells were transduced with A5 or A5M and treated with DOX (84 hours). Western blot analysis was carried out on whole-cell lysates with specific antibodies, as indicated. Different bands represent multiple C/EBPβ isoforms. (**D**) STAT3 and ERK1/ERK2 regulate C/EBPβ expression. TS-TTA cells were transduced with pLVTH-STAT3, pLVTH-ERK1 and pLVTH-ERK2, pLVTH-AKT1, or pLVTH-PLC–γ shRNA interfering constructs and treated with DOX (96 hours). Western blot analysis was carried out on whole-cell lysates with the specified antibodies. (**E**) C/EBPβ protein expression is restricted to ALK-positive ALCL cell lines. C/EBPβ and NPM-ALK expression was determined by Western blot analysis on a panel of lymphoma/leukemia cell lines. α-Tubulin protein expression was included for protein normalization.

cells (29), and its expression was very recently shown to be regulated by ALK in ALCL cells (30). We then decided to investigate whether C/EBPβ plays a pathogenetic role in ALK-driven transformation. We first investigated whether the GEP data confirmed this relationship in lymphoid and in nonlymphoid cells. *CEBPB* expression levels strongly covaried with *TNFSFR8* and with *ALK* expression in gene-silencing experiments (Figure 5B and Supplemental Figure 3A). Moreover, hierarchical clustering performed on the probe sets specific for *CEBP* family members showed that *CEBPB* was the gene with the most correlated expression profile to *NPM-ALK*, both in the TS and in Su-DHL1 cells (Supplemental Figure 3B). The link between *ALK* and *CEBPB* was further confirmed in an epithelial cell model (HEK-293T-Rex) in which NPM-ALK was ectopically expressed after doxycycline induction (Supplemental Figure 3, C–E).

To validate the microarray data, we carried out protein expression studies on ALCL cells using an antibody recognizing the C-terminal region of C/EBPβ and verified that the expression of C/EBPβ was strongly repressed following NPM-ALK RNAi both in the TS and Su-DHL1 cells (Figure 5C). We next asked which

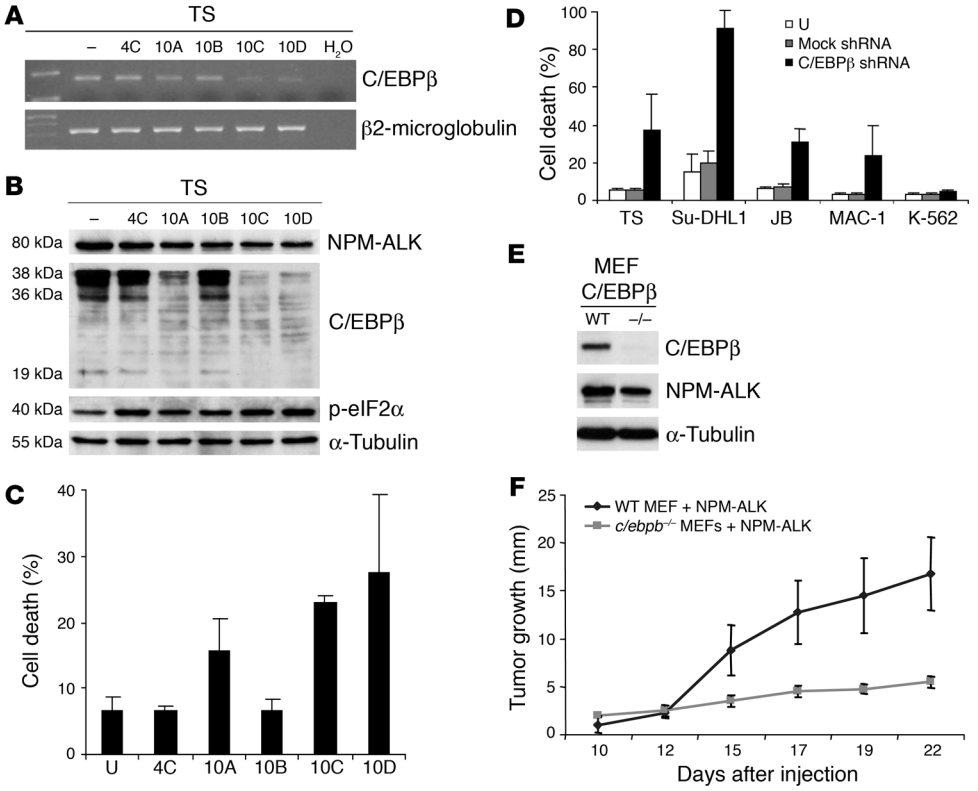

Figure 6
C/EBPβ is required for ALK-mediated transformation and tumor growth. (**A** and **B**) Downregulation of C/EBPβ expression by RNAi. TS cells were transduced with lentivirus (pLKO-GFP) expressing control (4C) or 4 C/EBPβ-directed shRNAs (10A–D). C/EBPβ mRNA and protein expression were determined by RT-PCR (**A**) and Western blot (**B**) analyses (96 hours). As a control, *β2-microglobulin* mRNA, α-tubulin, and phospho-eIF2α protein expression was documented. (**C** and **D**) C/EBPβ knock down compromises viability of ALCL cells in vitro. (**C**) TS cells were transduced with the indicated shRNA lentivirus. Percentage of apoptotic cells (sub-G_0/G_1) was determined by PI staining at day 5. (**D**) ALK-positive ALCL (TS, Su-DHL1, and JB) and ALK-negative (MAC-1 and K-562) cell lines were transduced with C/EBPβ (10D) or mock shRNA constructs. Apoptotic cells were determined at day 7. These findings are representative of 3 independent experiments. Error bars indicate SD. (**E** and **F**) C/EBPβ expression is required for tumor growth of ALK-positive cells in vivo. WT and *c/ebpb*$^{-/-}$ MEFs were transduced with a retrovirus expressing EGFP/NPM-ALK. NPM-ALK, C/EBPβ, and α-tubulin protein expression was determined by Western blotting (**E**) prior to subcutaneous inoculation (5×10^5 cells/mouse) into 8 athymic *nu/nu* mice recipients. Tumor growth was monitored over time (**F**). Error bars indicate SD.

signaling pathway(s) were responsible for NPM-ALK–mediated regulation of C/EBPβ in ALCL cells. To answer this question, we inhibited 4 critical pathogenetically relevant pathways of NPM-ALK signaling by specific shRNAs: ERK1/ERK2, STAT3, AKT1/AKT2, and PLC-γ. Using this approach, we observed that STAT3 silencing significantly downmodulated the expression of C/EBPβ, while ERK knock down resulted in a slight reduction in C/EBPβ protein levels (Figure 5D). To confirm these findings and to study the expression of C/EBPβ in hematopoietic cells, we carried out Western blot analysis on a broad panel of T and B lymphoma/leukemia cell lines. Three out of 4 ALK-positive ALCL cell lines demonstrated strong expression of C/EBPβ protein; less pronounced expression was found in the Karpas 299 cell line, whereas no detectable expression was seen in other cells, including an ALK-negative mature T cell line (MAC-1) (Figure 5E). These data were confirmed in a panel of primary human lymphomas in which strong C/EBPβ expression was demonstrated preferentially in ALK-positive ALCL samples (data not shown).

To assess the functional properties of C/EBPβ expression in ALCL cells, we silenced its expression by lentivirus-mediated RNAi. Among 4 independent C/EBPβ shRNA sequences, 3 led to downregulation of endogenous C/EBPβ RNA and protein levels, in which sequences 10C and 10D were the most effective. Several control shRNA sequences against irrelevant targets had no effect on C/EBPβ expression (Figure 6, A and B, and data not shown). We then verified whether shRNA-mediated knock down of C/EBPβ could affect tumor cell proliferation or viability in ALK-positive TS cells. Increased percentage of cell death was found to be proportional to the degree of C/EBPβ downregulation (Figure 6C and data not shown). To prove that the biological changes induced by C/EBPβ silencing were specific, we transduced 2 additional ALK-positive ALCL (Su-DHL1 and JB) and 2 *ALK*-negative cell lines (MAC-1 and K-562) with a C/EBPβ (sequence 1C) or a control shRNA and monitored the percentage of apoptotic cells. Downregulation of C/EBPβ led to a marked increase in apoptosis in all ALK-positive cell lines without any significant impairment of survival in the *ALK*-negative cell lines (Figure 6D).

We subsequently investigated whether C/EBPβ was required for NPM-ALK–mediated cellular transformation of mouse embryonic fibroblasts (MEFs). NPM-ALK–transduced WT and *c/ebpb*$^{-/-}$ MEFs were first evaluated for their cell growth ability following serum starvation. In these conditions, NPM-ALK expression induced cell-cycle progression of WT MEFs but failed to cause the entry into the S phase of *c/ebpb*$^{-/-}$ cells (data not shown). In vivo, *c/ebpb*$^{-/-}$ NPM-ALK MEFs injected into athymic *nu/nu* mice generated significantly smaller tumors compared with WT MEFs (Figure 6, E and F), underlining the relevance of C/EBPβ in sustaining the transforming properties of NPM-ALK.

Taken together, our analyses demonstrate that C/EBPβ expression is transcriptionally regulated by NPM-ALK mainly through STAT3 signaling. More importantly, C/EBPβ plays a crucial role in supporting both transformation and survival of NPM-ALK–positive cells.

Discussion

We have used GEP in association with a functional validation approach to identify the molecular mechanisms leading to NPM-

ALK lymphoid transformation and to discover key players that may represent feasible targets for ALCL therapies. To achieve this objective, we have adopted a loss-of-function approach with inducible lentivirus-mediated RNAi and potent ALK inhibitors in multiple human NPM-ALK–transformed lymphoid cell lines. This method produced a reliable and restricted expression signature of oncogenic ALK in the appropriate cellular context, and it cross-validated ALK inhibitor and shRNA-mediated approaches as therapeutic tools for treatment of ALK-positive ALCLs. Using a battery of lentiviral shRNA constructs, we assessed the pathogenetic role of ALK-regulated genes and their individual contribution to the generation and maintenance of ALK neoplastic phenotype, establishing that both BCL2A1 and C/EBPβ are necessary for sustaining the survival and/or growth of ALK-positive ALCL cells.

Gene expression studies have been widely used to stratify tumors and to identify informative signatures with the intent to discover pathogenetic molecules and/or pathways. We therefore decided to use this method in association with an RNAi strategy in ALK-positive ALCL cells. To analyze the effects of NPM-ALK expression in its native cellular background (ALCL), we used an inducible RNAi approach capable of silencing the expression of NPM-ALK fusion protein in ALK-positive cells. We have previously shown, using a constitutively expressed shRNA construct and small-molecule approach, that ALK expression is strictly required for the survival of ALK-positive ALCL cells in vitro and in vivo (11, 12). Here, we have further exploited this tool to generate ALK-positive cell lines expressing a doxycycline-inducible ALK shRNA. The expression of inducible ALK shRNA in time-controlled experimental conditions allowed us to identify a limited set of genes concordantly regulated by ALK, which are involved in cell cycle, proliferation, adhesion, mobility, signaling, inflammation, and transcriptional regulation. The inspection of expression profiling data revealed that ALK upregulates multiple genes related to neural differentiation even in lymphoid cells, consistent with its putative physiological role in the nervous system (31). Moreover, the upregulation of RHOB and other proteins involved in G protein signaling and migration suggests a molecular mechanism for the loose adhesion and aberrant anaplastic phenotype of ALK-positive ALCL cells (13).

To extend and corroborate our findings, we have compared the results of our microarray analyses with publicly available data. Despite the fact that signatures have previously been obtained using diverse approaches (serial analysis of gene expression [SAGE], subtractive suppression hybridization, or using a cDNA Atlas array), we were able to confirm a limited number of overlapping genes among these studies. These included *JUNB*, *MYC*, *BIRC5* (*survivin*), *CCND3* (*cyclin D3*), and *BCL3*. Nevertheless, the majority of the genes identified by our combined approach are novel. The differences among these studies may be due to many factors, including the limited number of samples, inappropriate ALK control cell lines and different technologies and modalities of evaluation. Notably, unbiased approaches can only identify end points of complex cancer-causing alterations. By exploiting a controlled loss-of-function approach relying on the experimental modulation of oncogene, we have been able to circumvent these problems.

Nevertheless, a loss-of-function method (whether by dominant-negative constructs, RNAi, or pharmacologic treatment) might suffer from lack of specificity (32). In particular, effects observed using shRNA might be due to the activation of interferon-mediated pathways and off-target silencing. To exclude these problems, we confirmed that ALK silencing was not linked to any significant induction of interferon-mediated genes and that a mutated ALK shRNA sequence (ALK-A5M) modulated a very limited number of target mRNAs. Last, to confirm the specificity of the RNAi profiles, we abrogated ALK activity with potent ALK inhibitors. This strategy allowed us to generate a bona fide ALK oncogenic signature by filtering out the genetic noise and the majority of off-target effects connected to the experimental system employed to inactivate ALK.

The combined use of GEP and RNAi technology has been demonstrated to be a valuable strategy to validate potential drug targets (33–35), and RNAi has been recently used to efficiently probe the gene function on a whole-genome scale in mammalian cells (36, 37). Here, ALK transcriptional targets were validated through a small-scale genetic screening, using lentiviral shRNA sequences. This screening identified several genes that promote growth and survival of tumor cells, both in cell culture and in animal models. Among them, we discovered BCL2A1 and C/EBPβ as critical mediators of NPM-ALK–dependent transformation and/or cell survival.

Human *BCL2A1* gene encodes for a BCL2 family protein whose expression in normal tissues is largely restricted to the hematopoietic compartment. In particular, BCL2A1 developmentally regulated in B and T cells, where it sustains the viability of T lymphoblasts (26, 38). In cancer cell lines, BCL2A1 is overexpressed in certain human epithelial and hematopoietic malignancies such as diffuse large B cell lymphoma and B cell chronic lymphocytic leukemia (39, 40). Using multiple approaches to inactivate ALK signaling in ALCL cells, we demonstrated that BCL2A1 is a specific NPM-ALK–regulated gene. In fact, ALK affects the expression of a limited number of *BCL2* family members, with *BCL2A1* and *BAX* the only 2 genes strictly correlated. We can envision a model in which NPM-ALK promotes survival, at least in part, through induction of *BCL2A1* and repression of *BAX* expressions. Given that *BCL2A1* expression is not affected by canonical ALK signaling molecules (data not shown), additional mediators should be pursued in order to identify the mechanisms of its regulation. Finally, since pathological BCL2A1 expression is not restricted to ALCL, its tumorigenic role may be more general, making this protein an appealing target for cancer therapy.

The findings on the role of C/EBPβ in ALCL cells are in agreement with previous reports describing its involvement in the promotion of proliferation (41), oncogene-mediated tumorigenesis (42), and apoptosis resistance (43). C/EBPβ levels are indeed increased in many tumors (44), and gene expression databases have established that C/EBPβ is an indispensable effector of cyclin D1 transcriptional activity (45). Here, we demonstrated that ALK regulates *CEBPB* transcription and its protein levels mainly through STAT3. This data are in accordance with the notion that the *CEBPB* promoter is regulated by several factors, such as CREB/ATF and Sp1 proteins, and by STAT3 itself, albeit indirectly, and is subject to a tight autoregulation (28). In conjunction with previously published observations on C/EBPβ expression in ALCL (29, 30), our data demonstrate for the first time to our knowledge an instrumental and pathogenetic role of C/EBPβ in promoting NPM-ALK oncogenesis.

Several findings have emerged regarding the mechanisms leading to ALK-mediated transformation. The data so far available suggest that ALK activation fires multiple signaling pathways; nonetheless, their individual contribution to ALK-mediated transformation remains quite unclear. In fact, the pathogenetic role of these pathways has not been documented in T cells but has been

extrapolated from studies using other models (e.g., BaF3, NIH3T3 cell lines). The only exception is STAT3 activation, the tumorigenic role of which is now well established in human and murine T cells (17). Based on previous and present findings, it is plausible that ALK transformation may be consequent to the activation of multiple players, each of them partially contributing to the oncogenic process. Many of these "weak" oncogenes such as *CEBPB* are regulated by STAT3. However, the contribution of additional pathways should be considered. In fact, we have demonstrated that molecules such as BCL2A1, which are not regulated either by STAT3 or other major ALK-mediated signaling pathways, play an important role. Moreover, it would be necessary to dissect the individual contribution of genes that are downregulated by ALK activity that could act as tumor suppressors. Only a systematic functional validation of all ALK transcriptional targets can conclusively solve this issue. Understanding of the precise contribution of these molecules may also serve to define novel therapeutic targets.

In conclusion, this study and others (46) demonstrate that it is possible to dissect the regulatory networks downstream of any oncogene within the appropriate cellular context by combining 2 of the most powerful new technologies in cancer research, RNAi and microarray analysis. A systematic functional screening should consequently allow the discovery of mechanisms and oncogenic pathways suitable for therapeutic targeting in cancers.

Methods

shRNA sequences, cDNA, and plasmid constructs. The shRNA utilized in this study (ALK-A5 shRNA) was directed against the cytoplasmic domain of ALK. The target sequence A5 is as follows: GGGCGAGCTACTATAGAAA; the A5M control sequence is mutated in 3 nucleotides (11). LV-shALK vectors were constructed by subcloning the H1 promoter–shALK cassette into the EcoRI-ClaI sites of the pLVTH vector (47), kindly provided by D. Trono (University of Geneva, Geneva, Switzerland). Additional shRNAs were obtained from the Expression Arrest TRC library (Open Biosystems) (37). The puromycin resistance gene was removed from the pLKO1 vector and replaced with a KpnI-BamHI fragment from pCCL containing EGFP-WPRE.

Cell culture, transfection, and retroviral and lentiviral infection. HEK293T cells were cultured under standard conditions (37°C in humidified atmosphere, with 5% CO_2) in DMEM supplemented with 10% FCS. Human ALK-positive ALCL (TS [a subclone of Sup-M2; ref. 11], Karpas 299, Su-DHL-1, JB), ALK-negative (MAC-1), acute lymphoblastic leukemia (Jurkat, CCRF-CEM), multiple myeloma (RPMI-8226, U-266), Burkitt lymphoma (BL-44, NAMALWA), chronic myeloid leukemia (K-562), and Hodgkin lymphoma (Sup-HD1, L540) cells were grown in RPMI 1640 medium with 10% FCS. Self-inactivating retroviral and lentiviral particles were produced as described previously (48). Aliquots of virus, plus 8 μg/ml polybrene, were used to infect exponentially growing cells (1×10^5/ml). Fresh medium was supplemented at 24 hours after infection. The infectivity was determined (after 72 hours) by FACS analysis of GFP-positive cells.

Generation of inducible cell lines. For conditional RNAi, cells were transduced at high efficiency with pLV-DsRed-tTRKRAB, expanded, and used for transduction with pLVTH-GFP-shRNA lentiviral particles. Next, the cells were treated with doxycycline (1 μg/ml) for 12 hours, double GFP^+DsRed^+ cells were sorted by MoFlo High-Performance fluorescence-activated cell sorting (Dako), and expanded. Cells expressing GFP in the absence of the inducer were considered "leaky" and removed by a second flow cytometry sorting. The inducible expression of NPM-ALK was obtained using the 293T-REx Tet-On system (Invitrogen) in HEK293 cells. NPM-ALK expression was induced by the presence of doxycycline (1 μg/ml).

Antibodies and Western blotting. The following primary antibodies were used for Western blotting as previously described (48): mouse anti-ALK (4C5B8) and mouse anti-STAT3 (5G7) from Zymed; mouse anti–α-tubulin (B-5-1-1) from Sigma-Aldrich; mouse anti–JunB (N-17), rabbit anti-ERK1 (C-16), rabbit anti-ERK2 (C-14), rabbit anti–PLC-γ (1249), rabbit anti-BCL2A1 (FL-175), and mouse anti-C/EBPβ (H-7) from Santa Cruz Biotechnology Inc.; rabbit anti–phospho-STAT3 Tyr705, rabbit anti–phospho-ALK Tyr1604, and rabbit anti-AKT from Cell Signaling Technology; mouse anti-TNFRSF8 from Dako; rabbit anti–phospho-eIF2α (Ab–1) from Oncogene Research; and rabbit anti-GFP from Invitrogen.

Total RNA isolation and biotin-labeled target preparation. Total RNA was extracted using the TRIzol reagent (Invitrogen) and purified using the RNeasy Mini kit (QIAGEN). The RNA integrity was verified by means of an Agilent Technologies 2100 Bioanalyzer. The biotin-labeled cRNA was synthesized as previously described (49). In accordance with the Affymetrix protocols, 15 μg of fragmented cRNA was hybridized on GeneChip Human Genome U133A Arrays (Affymetrix) after quality checking on GeneChip Test3 Arrays (Affymetrix). The oligonucleotide arrays were scanned using the Affymetrix GeneChip Scanner 3000 7G and images acquired using Microarray Suite (MAS) 5.0 software.

RT-PCR. cDNA was transcribed using SuperScript III (Invitrogen) following the manufacturer's instructions. PCR reactions were carried out for 25, 30, and 35 cycles and analyzed by gel electrophoresis and ethidium bromide staining as described previously (14). The reactions were performed in triplicate. The primer sequences were: β_2-MICROGLOBULIN, 5′-CTCGCGCTACTCTCTCTTTCTGG, 5′-GCTTACATGTCTCGATCCCACTTA; ICOS, 5′-GTGCTCACTGGGAGTGGAAT, 5′-GTCAACTGGGGTTCAGCAAT; RGS16, 5′-CCAGAACTCCAGGTTCTCCTCACTG, 5′-CACCTGCCTGGAGAGAGCCAAAGAG; CCL20, 5′-GCAAGCAACTTTGACTGCTG, 5′-TGGGCTATGTCCAATTCCAT; DKC1, 5′-GTTGACTACAGTGAGTCTGCC, 5′-ACCAGCTTTGGCCTTCTTGTCC; GNL3, 5′-GGATCCATGAAAAGGCCTAAGTTAAAGAAAGC, 5′-AAGCTTGCTCTCCAAATTCTCCTTTGGTA; BCL2A1, 5′-AGCCTACGCACGAAAGTGAC, 5′-TGTTGGCAATCGTTTCCATATC; CEBPB, 5′-ATCGACTTCAGCCCGTACCT, CCGTAGTCGTCGGAGAAGAG; TNFRSF8, 5′-CTGTGTCCCCTACCCAATCT, 5′-CTTCTTTCCCTTCCTCTTCCA; ALK, 5′-GGGCCATGGCGCCTTTGGGGAGGT, 5′-GTTGGGCCTGTCTTCAGGCTGATGTTG.

Microarray data analysis. The probe level data were converted to expression values using the MAS 5.0 algorithm and normalized using the "global scaling" procedure (49), which normalizes the signals of different experiments to the same target intensity. Unsupervised analyses were applied to a subset of genes whose average change in expression levels varied at least 2-fold from the mean across the whole panel. Hierarchical agglomerative clustering and dendrogram generation were used to search for natural groupings in the profiles using DNA-Chip Analyzer (dChip) software (25); in order to perform the clustering of the selected probe lists, Pearson's correlation coefficient and average linkage were used as distance and linkage methods, respectively (49, 50). The supervised gene expression analyses were performed using the Gene@Work software platform as previously described (49). Briefly, Gene@Work discovers global gene expression signatures that are common to an entire set of at least n experiments (the support set), where n was chosen as $n = n_0$; n_0 being the total number of samples in the set. Differentially expressed genes were identified by comparing expected gene expression probability densities, empirically computed from the experimental set with predefined threshold (51), and ranked according to statistical significance (gene z score). The data discussed in this publication have been deposited in the National Center for Biotechnology Information's Gene Expression Omnibus (GEO; http://www.ncbi.nlm.nih.gov/geo/) and are accessible through GEO Series accession number GSE6184.

Analysis of apoptosis by flow cytometry. Apoptosis was measured by flow cytometry after staining with annexin V or tetrametylrodamine methyl ester (TMRM). Annexin V binding was revealed by incubation with streptavidin-PE (11).

Tumor growth in immunocompromised mice. TS-TTA-A5 cells were injected (1×10^7) subcutaneously into the 2 rear flanks of 12 homozygous BNX (NIH-*Lyst*^{bg} *Foxn1*^{nu} *Prkdc*^{xid}) mice (Charles River Laboratories). Mice were treated with 0.1 mg/ml doxycycline in a 0.5% sucrose solution in light-proof bottles, refreshed every 4 days. WT and *cebpb*$^{-/-}$ MEFs were transduced with Pallino-NPM-ALK supernatants. The percentage of transduced cells was determined by FACS analysis of GFP-positive cells, and NPM-ALK expression was confirmed by Western blotting. GFP-positive MEFs (5×10^5) were injected subcutaneously into 8 athymic *nu/nu* mice (Charles River Laboratories). Tumor growth was monitored over time by determining the diameter of tumor masses. Animals used in this study were housed in the animal facility of the University of Turin School of Medicine and treated under guidelines approved by the Ethical Animal Committee of the same university.

Acknowledgments

We thank Didier Trono, Valeria Poli, and Andrea Califano for reagents and software; and Paola Bernabei, Andrea D. Manazza, and Valentina Grosso for technical help. This project was supported by NIH grant R01-CA64033; Sixth Research Framework Program of the European Union, Project RIGHT (LSHB-CT-2004-005276); Ministero dell'Università e Ricerca Scientifica (MIUR); Regione Piemonte; Compagnia di San Paolo, Torino (Progetto Oncologia); and Associazione Italiana per la Ricerca sul Cancro (AIRC). R. Piva is supported by the MIUR program "Incentivazione alla mobilità di studiosi residenti all'estero."

Received for publication June 15, 2006, and accepted in revised form September 26, 2006.

Address correspondence to: Giorgio Inghirami or Roberto Piva, Department of Pathology and CeRMS, University of Torino, Via Santena 7, Torino 10126 Italy. Phone: 39-011-6334623; Fax: 39-011-633-6500; E-mail: giorgio.inghirami@unito.it (G. Inghirami). Phone: 39-011-6336860; Fax: 39-011-633-6887; E-mail: roberto.piva@unito.it (R. Piva).

Roberto Piva and Elisa Pellegrino contributed equally to this work.

1. Morris, S.W., et al. 1994. Fusion of a kinase gene, ALK, to a nucleolar protein gene, NPM, in non-Hodgkin's lymphoma. *Science.* **263**:1281–1284.
2. Duyster, J., Bai, R.Y., and Morris, S.W. 2001. Translocations involving anaplastic lymphoma kinase (ALK). *Oncogene.* **20**:5623–5637.
3. Kutok, J.L., and Aster, J.C. 2002. Molecular biology of anaplastic lymphoma kinase-positive anaplastic large-cell lymphoma. *J. Clin. Oncol.* **20**:3691–3702.
4. Pulford, K., Morris, S.W., and Turturro, F. 2004. Anaplastic lymphoma kinase proteins in growth control and cancer. *J. Cell. Physiol.* **199**:330–358.
5. Lamant, L., et al. 2000. Expression of the ALK tyrosine kinase gene in neuroblastoma. *Am. J. Pathol.* **156**:1711–1721.
6. Cessna, M.H., et al. 2002. Expression of ALK1 and p80 in inflammatory myofibroblastic tumor and its mesenchymal mimics: a study of 135 cases. *Mod. Pathol.* **15**:931–938.
7. Lu, K.V., et al. 2005. Differential induction of glioblastoma migration and growth by two forms of pleiotrophin. *J. Biol. Chem.* **280**:26953–26964.
8. Morris, S.W., et al. 1997. ALK, the chromosome 2 gene locus altered by the t(2;5) in non-Hodgkin's lymphoma, encodes a novel neural receptor tyrosine kinase that is highly related to leukocyte tyrosine kinase (LTK). *Oncogene.* **14**:2175–2188.
9. Iwahara, T., et al. 1997. Molecular characterization of ALK, a receptor tyrosine kinase expressed specifically in the nervous system. *Oncogene.* **14**:439–449.
10. Chiarle, R., et al. 2003. NPM-ALK transgenic mice spontaneously develop T-cell lymphomas and plasma cell tumors. *Blood.* **101**:1919–1927.
11. Piva, R., et al. 2006. Ablation of oncogenic ALK is a viable therapeutic approach for anaplastic large-cell lymphomas. *Blood.* **107**:689–697.
12. Wan, W., et al. 2006. Anaplastic lymphoma kinase activity is essential for the proliferation and survival of anaplastic large-cell lymphoma cells. *Blood.* **107**:1617–1623.
13. Ambrogio, C., et al. 2005. p130Cas mediates the transforming properties of the anaplastic lymphoma kinase. *Blood.* **106**:3907–3916.
14. Zamo, A., et al. 2002. Anaplastic lymphoma kinase (ALK) activates Stat3 and protects hematopoietic cells from cell death. *Oncogene.* **21**:1038–1047.
15. Slupianek, A., et al. 2001. Role of phosphatidylinositol 3-kinase-Akt pathway in nucleophosmin/anaplastic lymphoma kinase-mediated lymphomagenesis. *Cancer Res.* **61**:2194–2199.
16. Wellmann, A., et al. 1997. The activated anaplastic lymphoma kinase increases cellular proliferation and oncogene up-regulation in rat 1a fibroblasts. *FASEB J.* **11**:965–972.
17. Chiarle, R., et al. 2005. Stat3 is required for ALK-mediated lymphomagenesis and provides a possible therapeutic target. *Nat. Med.* **11**:623–629.
18. Rassidakis, G.Z., et al. 2005. Inhibition of Akt increases p27Kip1 levels and induces cell cycle arrest in anaplastic large cell lymphoma. *Blood.* **105**:827–829.
19. Bai, R.Y., Dieter, P., Peschel, C., Morris, S.W., and Duyster, J. 1998. Nucleophosmin-anaplastic lymphoma kinase of large-cell anaplastic lymphoma is a constitutively active tyrosine kinase that utilizes phospholipase C-gamma to mediate its mitogenicity. *Mol. Cell. Biol.* **18**:6951–6961.
20. Villalva, C., et al. 2002. Isolation of differentially expressed genes in NPM-ALK-positive anaplastic large cell lymphoma. *Br. J. Haematol.* **118**:791–798.
21. Wellmann, A., et al. 2000. Detection of differentially expressed genes in lymphomas using cDNA arrays: identification of clusterin as a new diagnostic marker for anaplastic large-cell lymphomas. *Blood.* **96**:398–404.
22. Rust, R., et al. 2005. High expression of Mcl-1 in ALK positive and negative anaplastic large cell lymphoma. *J. Clin. Pathol.* **58**:520–524.
23. Willenbrock, K., et al. 2006. Common features and differences in the transcriptome of large cell anaplastic lymphoma and classical Hodgkin's lymphoma. *Haematologica.* **91**:596–604.
24. Watanabe, M., et al. 2005. JunB induced by constitutive CD30-extracellular signal-regulated kinase 1/2 mitogen-activated protein kinase signaling activates the CD30 promoter in anaplastic large cell lymphoma and reed-sternberg cells of Hodgkin lymphoma. *Cancer Res.* **65**:7628–7634.
25. Schadt, E.E., Li, C., Ellis, B., and Wong, W.H. 2001. Feature extraction and normalization algorithms for high-density oligonucleotide gene expression array data. *J. Cell. Biochem. Suppl.* **37**:120–125.
26. Mandal, M., et al. 2005. The BCL2A1 gene as a pre-T cell receptor-induced regulator of thymocyte survival. *J. Exp. Med.* **201**:603–614.
27. Ferrando, A.A., et al. 2002. Gene expression signatures define novel oncogenic pathways in T cell acute lymphoblastic leukemia. *Cancer Cell.* **1**:75–87.
28. Ramji, D.P., and Foka, P. 2002. CCAAT/enhancer-binding proteins: structure, function and regulation. *Biochem. J.* **365**:561–575.
29. Jundt, F., et al. 2005. A rapamycin derivative (everolimus) controls proliferation through down-regulation of truncated CCAAT enhancer binding protein beta and NF-kappaB activity in Hodgkin and anaplastic large cell lymphomas. *Blood.* **106**:1801–1807.
30. Quintanilla-Martinez, L., et al. 2006. NPM-ALK dependent expression of the transcription factor CCAAT/enhancer binding protein (C/EBP)beta in Alk-positive anaplastic large cell lymphomas. *Blood.* **108**:2029–2036.
31. Pulford, K., et al. 2004. The emerging normal and disease-related roles of anaplastic lymphoma kinase. *Cell. Mol. Life Sci.* **61**:2939–2953.
32. Jackson, A.L., et al. 2003. Expression profiling reveals off-target gene regulation by RNAi. *Nat. Biotechnol.* **21**:635–637.
33. Yamamoto, A., Cremona, M.L., and Rothman, J.E. 2006. Autophagy-mediated clearance of huntingtin aggregates triggered by the insulin-signaling pathway. *J. Cell Biol.* **172**:719–731.
34. Kolfschoten, I.G., et al. 2005. A genetic screen identifies PITX1 as a suppressor of RAS activity and tumorigenicity. *Cell.* **121**:849–858.
35. Ngo, V.N., et al. 2006. A loss-of-function RNA interference screen for molecular targets in cancer. *Nature.* **441**:106–110.
36. Westbrook, T.F., et al. 2005. A genetic screen for candidate tumor suppressors identifies REST. *Cell.* **121**:837–848.
37. Moffat, J., et al. 2006. A lentiviral RNAi library for human and mouse genes applied to an arrayed viral high-content screen. *Cell.* **124**:1283–1298.
38. Tomayko, M.M., et al. 1999. Expression of the Bcl-2 family member A1 is developmentally regulated in T cells. *Int. Immunol.* **11**:1753–1761.
39. Mahadevan, D., et al. 2005. Transcript profiling in peripheral T-cell lymphoma, not otherwise specified, and diffuse large B-cell lymphoma identifies distinct tumor profile signatures. *Mol. Cancer Ther.* **4**:1867–1879.
40. Morales, A.A., et al. 2005. High expression of bfl-1 contributes to the apoptosis resistant phenotype in B-cell chronic lymphocytic leukemia. *Int. J. Cancer.* **113**:730–737.
41. Greenbaum, L.E., et al. 1998. CCAAT enhancer-binding protein β is required for normal hepatocyte proliferation in mice after partial hepatectomy. *J. Clin. Invest.* **102**:996–1007.
42. Zhu, S., Yoon, K., Sterneck, E., Johnson, P.F., and Smart, R.C. 2002. CCAAT/enhancer binding protein-beta is a mediator of keratinocyte survival and

skin tumorigenesis involving oncogenic Ras signaling. *Proc. Natl. Acad. Sci. U. S. A.* **99**:207–212.
43. Buck, M., Poli, V., Hunter, T., and Chojkier, M. 2001. C/EBPbeta phosphorylation by RSK creates a functional XEXD caspase inhibitory box critical for cell survival. *Mol. Cell.* **8**:807–816.
44. Zahnow, C.A. 2002. CCAAT/enhancer binding proteins in normal mammary development and breast cancer. *Breast Cancer Res.* **4**:113–121.
45. Lamb, J., et al. 2003. A mechanism of cyclin D1 action encoded in the patterns of gene expression in human cancer. *Cell.* **114**:323–334.
46. Smith, R., et al. 2006. Expression profiling of EWS/FLI identifies NKX2.2 as a critical target gene in Ewing's sarcoma. *Cancer Cell.* **9**:405–416.
47. Wiznerowicz, M., and Trono, D. 2003. Conditional suppression of cellular genes: lentivirus vector-mediated drug-inducible RNA interference. *J. Virol.* **77**:8957–8961.
48. Piva, R., et al. 2005. 15-Deoxy-delta 12,14-prostaglandin J2 induces apoptosis in human malignant B cells: an effect associated with inhibition of NF-kappa B activity and down-regulation of antiapoptotic proteins. *Blood.* **105**:1750–1758.
49. Mattioli, M., et al. 2005. Gene expression profiling of plasma cell dyscrasias reveals molecular patterns associated with distinct IGH translocations in multiple myeloma. *Oncogene.* **24**:2461–2473.
50. Eisen, M.B., Spellman, P.T., Brown, P.O., and Botstein, D. 1998. Cluster analysis and display of genome-wide expression patterns. *Proc. Natl. Acad. Sci. U. S. A.* **95**:14863–14868.
51. Jagasia, M., et al. 2004. Histology impacts the outcome of peripheral T-cell lymphomas after high dose chemotherapy and stem cell transplant. *Leuk. Lymphoma.* **45**:2261–2267.